Influence of δ doping position on subband properties in $In_{0.2}Ga_{0.8}As$/GaAs heterostructures

Zhiming Huang,[1,*] Roger Yu,[2] Chunping Jiang,[1] Tie Lin,[1] Zhanhong Zhang,[1] and Junhao Chu[1]
[1]*National Laboratory for Infrared Physics, Shanghai Institute of Technical Physics, Chinese Academy of Sciences, 420 Zhong Shan Bei Yi Road, Shanghai, 200083, People's Republic of China*
[2]*School of Natural Sciences, St. Edward's University, 3001 South Congress Avenue, Austin, Texas, 78704-6489*
(Received 10 April 2001; revised manuscript received 4 June 2001; published 10 May 2002)

Subband properties of Si δ-doped pseudomorphic $In_{0.2}Ga_{0.8}As$/GaAs heterostructures have been investigated by solving the Schrödinger-Kohn-Sham equation and the Poission equation self-consistently, and by the density-density dynamical response function. The shift of the same Si δ-doped layer from the quantum-well center (the origin is at 0 Å) to the barrier (310 Å) has been studied to find its effect on subband electron densities and mobilities. The electron density of the first subband is greater than 3.6×10^{12} cm^{-2} when a δ-doped density of 4.5×10^{12} cm^{-2} is placed in the well. It is only 2.06×10^{12} cm^{-2} for the doping position with a 85-Å spacer layer. The electron occupation of the second subband is 15.4% in the well-center-doped structure. It is up to the maximum of 42.3% at 130 Å. The electron mobility is not changed significantly for the first subband, but is varied noticeably for the second subband by moving the Si δ doping position in the well. The highest electron mobility is obtained at about 110 Å for the first subband, and at about 290 Å for the second subband. The calculated results are also compared to the corresponding experimental data.

DOI: 10.1103/PhysRevB.65.205312 PACS number(s): 73.21.−b, 71.15.Pd, 72.10.Di, 73.20.Mf

I. INTRODUCTION

Heterostructures based on materials in the III-V and III-V nitride families have been studied extensively for high speed and optoelectronic applications.[1–7] There has been a great interest in combining a delta doping (δ doping) with a heterostructure-based quantum well to improve the electrical transport properties of the systems.[8–12] The δ-doped layer can be placed at the center of the well, which can achieve high carrier densities in the well but produces limited electron mobilities because the charge carriers and impurities share the same region of space. The δ-doped layer can also be placed outside the well, or in the barrier region, to achieve higher mobilities owing to the fact that the mobile charge carriers are separated from the ionized impurities. Although different δ-doping configurations, in which δ-doped layers were placed at different positions with respect to the quantum well, have been tried experimentally to optimize the position of the δ-doped layer,[11,13–16] the relation of subband transport properties with the shift of the δ-doping position is not clear. In this paper, we investigate, as an example, the subband electrical properties of Si δ-doped pseudomorphic $In_{0.2}Ga_{0.8}As$/GaAs heterostructures by changing the doping position from the well center to the barrier (0–310 Å). Both the subband electron densities and mobilities of the first and second subbands are studied as a function of the doping position.

II. EXPERIMENTAL AND THEORETICAL MODEL

Si δ-doped $In_{0.2}Ga_{0.8}As$/GaAs heterostructures were grown in low-pressure (76 Torr) metalorganic vapor phase epitaxy at 630°C. The precursors included trimethylgallium (TMGa), trimethylindium (TMIn), and 100% AsH_3. The carrier gas was H_2 and the doping precursor was 500-ppm SiH_4 diluted in H_2. The growth rate was 2 μm/h for GaAs and 1.2 μm/h for $In_{0.2}Ga_{0.8}As$. (100)-oriented with 2° off toward the (110) semi-insulating GaAs wafers were used as substrates. The details of Si δ doping have been described elsewhere.[17]

The $In_{0.2}Ga_{0.8}As$/GaAs heterostructures studied in this paper are of the same Si δ-doped layer placed from the $In_{0.2}Ga_{0.8}As$ well center to the barrier. However the basic $In_{0.2}Ga_{0.8}As$/GaAs heterostructures, such as the well composition and thickness, are kept identical. The width of the quantum well is 100 Å. Therefore, position (A) at the well center is 0 Å, position (B) at the well-barrier interface is 50 Å, and position (C) is 200 Å with a 150-Å GaAs spacer layer. The Si δ-doped electron density is taken as 4.5×10^{12} cm^{-2} per layer.

To check our calculations, three Si δ-doped $In_{0.2}Ga_{0.8}As$/GaAs heterostructures corresponding to the above structures [(A)–(C)] were grown, respectively. Shubnikov–de Haas (SdH) measurements were made over the magnetic field range of 0–12 Tesla at 1.5 K. The samples were in Hall bar geometry with alloyed Au-Ge Ohmic contacts.

In order to understand the electron properties of the present many-electron systems, one needs to solve the Kohn-Sham Schrödinger equation

$$\left[-\frac{\hbar^2}{2m^*}\frac{d^2}{dz^2}+V_{eff}(z)\right]\phi_\alpha(z)=E_\alpha\phi_\alpha(z), \qquad (1)$$

in conjunction with the Poission equation, self-consistently.[18] In the above equation, z is the coordinate along the growth direction, $V_{eff}(z)$ is the effective potential which contains (1) the Hartree potential $v_H(z)$, (2) the exchange and correlation potential $v_{xc}(z)$ of Hedin and Lundqvist,[19] (3) the background potential profile $E_b(z)$, and (4) the potential energy due to strain effects.[20] The subband charge densities n_α, wave functions ϕ_α, energy levels E_α, and Fermi energy E_F for the interacting inhomogeneous electron gas can be

 ©2002 The American Physical Society

well described within the framework of the effective-mass approximation. The details of the calculation procedure have been given elsewhere.[21]

The dynamical response of the inhomogeneous electron system is described by the density-density correlation function $\chi(q_\parallel,\omega;z,z')$, which can be obtained by solving a Dyson-type integral equation

$$\chi(q_\parallel,\omega;z,z')=\chi^0(q_\parallel,\omega;z,z')-\int_0^L\int_0^L dz_1dz_2\chi^0 \times(q_\parallel,\omega;z,z_1)V(q_\parallel,z_1,z_2)\chi(q_\parallel,\omega;z_2,z'), \tag{2}$$

where L is the length of the heterostructures, $\chi^0(q_\parallel,\omega;z,z')$ is the response function of the noninteracting electron system, and $V(q_\parallel,z_1,z_2)$ is the electron-electron interaction potential.[22] The noninteracting response function $\chi^0(q_\parallel,\omega;z,z')$ is defined by

$$\chi^0(q_\parallel,\omega;z,z') = \sum_{\alpha=1}^{occ}\sum_{\alpha'=1}^{all} S_{\alpha,\alpha'}(q_\parallel,\omega)\phi_\alpha(z)\phi_\alpha(z')\phi_{\alpha'}(z)\phi_{\alpha'}(z'), \tag{3}$$

where the matrix $S_{\alpha,\alpha'}(q_\parallel,\omega)$ reads

$$S_{\alpha,\alpha'}(q_\parallel,\omega)=2\int_0^\infty \frac{d^2\mathbf{k}_\parallel}{(2\pi)^2}\frac{f(E_{k_\parallel,\alpha})-f(E_{k_\parallel+q_\parallel,\alpha'})}{E_{k_\parallel+q_\parallel,\alpha'}-E_{k_\parallel,\alpha}+i\Gamma}. \tag{4}$$

In the above equation, Γ is the phenomenological damping parameter, which is provided mainly by ionized impurity scattering at low temperatures and determined by sample quality. Usually, the value of the damping parameter at the δ-doped position is greater than that outside the doped position due to high-density δ doping. In our calculations, $\Gamma=4.0k_BT$, $2.2k_BT$ (k_B being the Boltzmann constant and T the experimental temperature) are assumed at and outside the Si δ-doped position, respectively. f is the Fermi-Dirac distribution function. The in-plane wave vector $q_\parallel$ has been chosen to be very small, $q_\parallel L\simeq 1$, to explore the dynamical response of the entire nonuniform electron gas.[23,24]

It is important to note that the α summation in Eq. (3) runs over the individual occupied states whereas the α' summation includes all possible states. The dynamical polarizability $p(q_\parallel,\omega)$ is related to the response function χ through the equation[25]

$$p(q_\parallel,\omega)=\int_0^L\int_0^L dz dz' \exp[-q_\parallel(z+z')]\chi(q_\parallel,\omega;z,z'), \tag{5}$$

in which an exponentially decaying external driving field $V_{ext}\sim e^{-q_\parallel z-i\omega t}$ was assumed.

The dynamical conductivity σ_α of the αth subband is given by using the dynamical polarizability $p(\omega)$ through the following equation:[26]

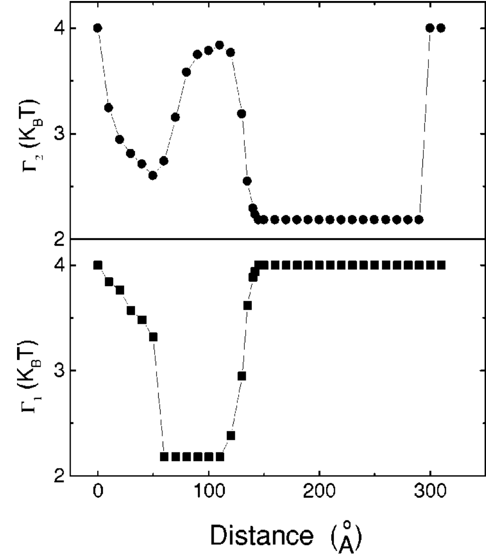

FIG. 1. Γ values of the first and second subbands as a function of Si δ doping position for InGaAs/GaAs heterostructures at 1.5 K. The well center is at 0 and the heterointerface at 50 Å.

$$\sigma_\alpha=\omega\,\mathrm{Im}[p(\omega)]. \tag{6}$$

Then the electron mobility μ_α of the αth subband can be obtained by

$$\mu_\alpha=\sigma_\alpha d_\alpha/en_\alpha, \tag{7}$$

where e is the electron charge, and d_α is the full electron density profile width at the half-maximum of the αth subband.

III. RESULTS AND DISCUSSION

In our calculations we only consider the lowest two subbands ($\alpha=1$ for the first subband and $\alpha=2$ for the second subband), due to the fact that they are occupied by most of the doping electrons. Figure 1 shows the phenomenological damping parameters Γ_α of the first and second subbands. The damping parameters Γ_α are defined by the spatial overlap between the wave function $\phi_\alpha(z)$ and the self-consistent potential $V_{eff}(z)$. The wave function $\phi_\alpha(z)$ shares partially at and outside the δ-doped position. Therefore, Γ_α comes from two components: one is the damping at the δ-doped position and the other is that outside the position. That is, when $\phi_\alpha(z)$ distributes both at and outside the δ-doped position, Γ_α is between $4.0k_BT$ and $2.2k_BT$. If Γ_α is taken as $4.0k_BT$, which means that $\phi_\alpha(z)$ is localized completely at the δ-doped position. Also, if Γ_α is $2.2k_BT$, this means that the wave function distributes outside the δ-doped position. As shown in Fig. 1, Γ_1 decreases from $4.0k_BT$ to $3.3k_BT$ and Γ_2 to $2.6k_BT$, respectively, when the δ-doping position layer is changed from the well center (0 Å) to the well-barrier interface (50 Å). This indicates that the wave functions of the first and second subbands depart little by little from the ionized Si donors. Next Γ_1 remains at a constant value of $2.2k_BT$ between 60 and 110 Å, where the wave function of the first subband is separated from the ionized Si donors.

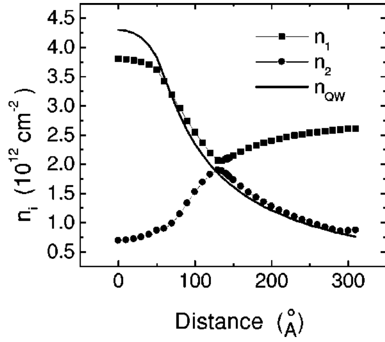

FIG. 2. The electron densities of the first and second subbands and in the $In_{0.2}Ga_{0.8}As$ quantum well as a function of Si δ doping position for $In_{0.2}Ga_{0.8}As/GaAs$ heterostructures at 1.5 K. The well center is at 0 and the heterointerface at 50 Å.

Then Γ_1 increases suddenly when the distance is over 120 Å, because the wave function of the first subband electrons begins to overlap again with the ionized donors. The wave function overlaps completely with the ionized impurities above 145 Å . Conversely, Γ_2 increases between 60 and 110 Å, then drops to $2.2k_BT$ at about 145 Å, due to the change of the spatial overlapping degree of its wave function with the doping position. The electrons of the second subband are also separated completely in space between 145 and 290 Å. However, Γ_2 increases to $4.0k_BT$ when the δ doping position is beyond 300 Å, because the δ-doping position is far away from the quantum well and the electron of the second subband cannot transfer into the well. Therefore, its wave function is localized completely at the Si donors.

The calculated electron densities of the first and second subbands n_1 and n_2 and in the $In_{0.2}Ga_{0.8}As$ quantum well n_{QW} are displayed in Fig. 2. It can be seen clearly that the first subband is heavily occupied by more than 80% of the doping electrons in the well-doped structures. The population is 3.8×10^{12} cm^{-2} for the well-center-doped structure. Then n_1 drops when the δ doping is placed away from the well center. A minimum electron density of 2.06×10^{12} cm^{-2} is obtained at the position of 135 Å , i.e., with a 85-Å spacer layer. The occupation of the first subband increases slowly as the doping position is shifted further away from the well center. The electron density of the second subband n_2 is only 15.4% of the doping concentration in the well-center doping structure, rises to a maximum of 42.3% at 130 Å, then drops to 19% at 290 Å. The total electron density n_{QW} in the well is 4.30×10^{12} cm^{-2} for the well-center-doped structure, then decreases to 4.03×10^{12} cm^{-2} for the well-barrier-interface structure. In the modulation-doped structures, n_{QW} drops when the δ-doping position moves away from the well center. The quantum well is occupied only by the first subband when the distance is between 60 and 110 Å, by a mixture of the lowest two subbands between 120 and 145 Å , and by the second subband alone between 145 and 290 Å.

Figure 3 shows the calculated conduction band profiles and the square of the electron wave functions for the first and second subbands of structures (A)–(C). For the well-center-doped structure (A) and the well-barrier-interface-doped structure (B), the first and second subbands are mainly in the

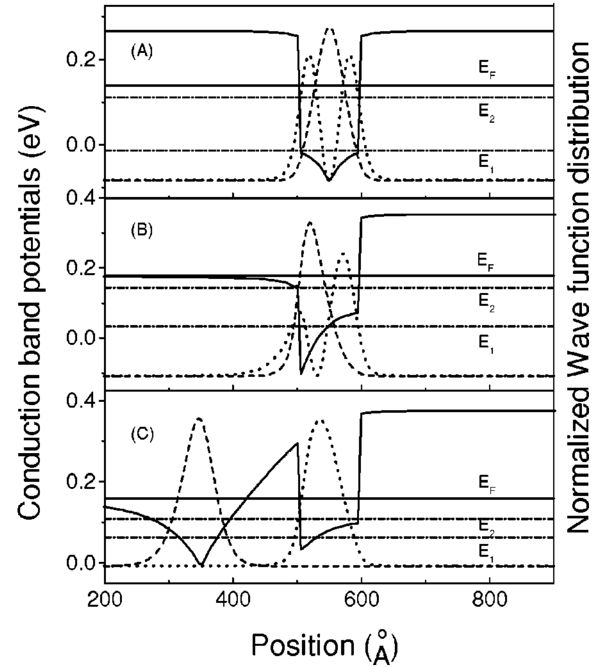

FIG. 3. The calculated conduction band and the square of the electron wave functions of the first subband (dashed lines) and second subband (dotted lines) as a function position at 1.5 K for (A) well center doping, (B) well-barrier interface doping, and (C) barrier layer doping with a 150 Å spacer layer.

quantum well. However, for the barrier-doped system (C), the first subband resides in the barrier region since the δ doping itself brings a deep and wide V-shaped well ino the GaAs barrier region; the second subband principally resides in the quantum well.

The mobilities of the lowest two subbands μ_1 and μ_2 are depicted in Fig. 4 as a function of the δ-doping position. The electron mobility of the first subband μ_1 is not changed much for different well-doped structures. It increases rapidly when the δ doping is beyond 60 Å, because the electron wave function of the first subband is spatially separated from the ionized Si donors. The wave function is completely sepa-

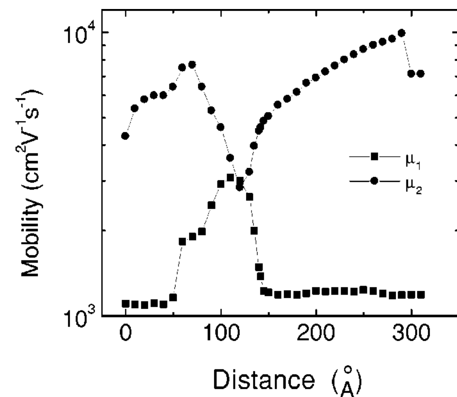

FIG. 4. The electron mobilities of the first and second subbands as a function of Si δ doping position for $In_{0.2}Ga_{0.8}As/GaAs$ heterostructures at 1.5 K. The well center is at 0 and the heterointerface at 50 Å.

TABLE I. The theoretical and experimental values of the electron densities and mobilities of the first and second subbands for Si δ-doped $In_{0.2}Ga_{0.8}As/GaAs$ heterostructures for (A) well center doping, (B) well-barrier interface doping, and (C) barrier layer doping with a 150 Å spacer layer at 1.5 K. The electron densities are in the unit of 10^{12} cm^{-2}, and the mobilities in the unit of $cm^2\,V^{-1}\,s^{-1}$.

	n_1		n_2		μ_1		μ_2	
Sample	Theory	Expt.	Theory	Expt.	Theory	Expt.	Theory	Expt.
A	3.80	3.78	0.70	—	1102	1120	4293	—
B	3.62	3.48	0.86	0.84	1159	1260	6402	4460
C	2.40	—	1.28	1.24	1220	—	6894	6900

rated from the ionized donors between 60 and 110 Å in terms of the Γ_1 values shown in Fig. 1, however, the impurity scattering is reduced further, which improves the mobility, when the position of the Si donors is moved away from the well.[27] μ_1 reaches the highest value of about 3100 $cm^2\,V^{-1}\,s^{-1}$ at about 110 Å, then decreases due to an increase in Γ_1. μ_1 remains almost constant beyond 145 Å, and the electrons of the first subband are located in the deep V-shaped potential well formed in the Si δ-doped layer. The electron mobility of the second subband μ_2 increases from 0 Å to 70 Å, then decreases to the lowest value of about 2800 $cm^2\,V^{-1}\,s^{-1}$ at 120 Å due to the fact that Γ_2 increases. Next μ_2 increases because the scattering becomes small. The highest mobility of the second subband can be obtained at a position of 290 Å. Finally, μ_2 drops when the distance is over 300 Å, where the wave function of the second subband is overlapped completely with the ionized Si donors.

To testify to our calculations, we measured the longitudinal resistivity (ρ_{xx}) of the $In_{0.2}Ga_{0.8}As/GaAs$ heterostructures with 4.5×10^{12} cm^{-2} Si δ-doped layers as a function of magnetic field for three different doping positions mentioned above. The fast Fourier transform analysis was applied to estimate the subband electron densities and mobilities.[28] The results are summarized in Table I. An excellent agreement is obtained between the theoretical and experimental data for the lowest two subband electron densities and mobilities of all configurations. The absence of n_1 and μ_1 in sample (C) from the SdH measurement has a simple interpretation: The wave function of the first subband has a maximum probability density with the delta-doped layer. It can be expected to have a poorer mobility than the calculated one. Therefore, the first subband cannot be picked up by the SdH effect. The electron density n_1 of the well-barrier-interface structure is slightly lower than the theoretical data, possibly due to the well-barrier-interface scattering effect of the sample.

IV. CONCLUSION

The influence of the Si δ-doping position on the subband electrical properties of pseudomorphic $In_{0.2}Ga_{0.8}As/GaAs$ heterostructures has been studied using self-consistent calculation, and the dynamical polarizability by shifting the doping position from the well center to the barrier step by step. Both the subband electron densities and mobilities have been obtained from the calculations. The first subband is heavily occupied with greater than 80% of the doping electrons in the well-doped structures. The minimum electron density of 2.06×10^{12} cm^{-2} is obtained at a position of 135 Å. The occupation of the second subband is only 15.4% of the doping density in the well-center structure; it goes up to the maximum of 42.3% at 130 Å, then down slowly to 19% at 290 Å. The quantum well is occupied only by the first subband between 60 and 110 Å, by a mixture of the lowest two subbands between 120 and 145 Å, and by the second subband alone before 290 Å in the modulation-doped structures. The electron mobility of the first subband is not changed much for the different well-doped structures. It reaches the highest value at about 110 Å, and remains almost constant beyond 145 Å. The lowest value of electron mobility of the second subband is at 120 Å, and the highest mobility can be obtained at the position of 290 Å. Our results show that the subband electron mobilities can be completely determined only by the damping parameters at and outside the δ-doping position. The calculated results are confirmed by the corresponding experimental data. Similar calculations can also be applied to other group-III-V and -III-nitride semiconductors to design and optimize device structures.

ACKNOWLEDGMENTS

The authors would like to acknowledge Professor R. Fu, W. Lu, and Dr. X. G. Wang for their helpful discussions. This work was supported by the National Nature Science Foundation of China (Grant No. 69738020).

*Electronic mail: zmhuang@public4.sta.net.cn

[1] T. R. Block, M. Wojtowicz, A. C. Han, S. R. Olson, A. K. Oki, and D. C. Streit, J. Vac. Sci. Technol. B **16**, 1475 (1998).
[2] Y. F. Zhang and J. Singh, J. Appl. Phys. **85**, 587 (1999).
[3] V. G. Mokerov, Y. V. Fedorov, and A. V. Hook, Fiz. Tekh. Poluprovodn. **33**, 1064 (1999) [Semiconductors **33**, 970 (1999)].
[4] T. Wang, J. Bai, S. Sakai, Y. Ohno, and H. Ohno, Appl. Phys. Lett. **76**, 2737 (2000).
[5] A. T. Schremer, J. A. Smart, Y. Wang, O. Ambacher, N. C. MacDonald, and J. R. Shealy, Appl. Phys. Lett. **76**, 736 (2000).
[6] J. J. Rosenberg, M. Benlamri, P. D. Kirchner, J. M. Woodall, and G. D. Pettit, IEEE Electron Device Lett. **EDL-6**, 491 (1985).

[7] A. Ketterson, M. Moloney, W. T. Masselink, C. K. Peng, J. Klem, R. Fischer, W. Kopp, and H. Morkoc, IEEE Electron Device Lett. **EDL-6**, 628 (1985).
[8] W. T. Masselink, Phys. Rev. Lett. **66**, 1513 (1991).
[9] W. T. Masselink, Appl. Phys. Lett. **59**, 694 (1991).
[10] M. L. Ke, D. Westwood, R. H. Williams, and M. J. Godfrey, Phys. Rev. B **51**, 5038 (1995).
[11] L. Bouzaiene, L. Sfaxi, H. Sghaeir, and H. Maaref, J. Appl. Phys. **85**, 8223 (1999).
[12] G. Y. Zhao, M. Adachi, H. Ishikawa, T. Egawa, M. Umeno, and T. Jimbo, Appl. Phys. Lett. **77**, 2195 (2000).
[13] Y. J. Jeon, Y. H. Jeong, B. Kim, Y. G. Kim, W. P. Hong, and M. S. Lee, IEEE Electron Device Lett. **16**, 563 (1995).
[14] M. J. Kao, W. C. Hsu, and C. Y. Chang, Jpn. J. Appl. Phys., Part 2 **34**, L1 (1995).
[15] W. C. Hsu, C. L. Wu, M. S. Hsai, C. Y. Chang, W. C. Wu, and H. M. Shieh, IEEE Trans. Electron Devices **42**, 802 (1995).
[16] J. Dickmann, Appl. Phys. Lett. **60**, 88 (1992).
[17] G. Li, C. Jagadish, M. B. Johnston, and M. Gal, Appl. Phys. Lett. **69**, 4218 (1996).
[18] W. Kohn and L. J. Sham, Phys. Rev. **140**, A1133 (1965).
[19] L. Hedin and B. I. Lundqvist, J. Phys. C **4**, 2064 (1971).
[20] J. M. Gilpérez, J. L. Sánchez-Rojas, E. Muñoz, E. Calleja, J. P. R. David, M. Reddy, G. Hill, and J. Sánchez-Dehesa, J. Appl. Phys. **76**, 5931 (1994).
[21] Roger H. Yu, Phys. Rev. B **47**, 15692 (1993).
[22] Roger H. Yu, Phys. Rev. B **47**, 1379 (1993).
[23] D. H. Ehlers and D. L. Mills, Phys. Rev. B **34**, 3939 (1986).
[24] S. R. Streight and D. L. Mills, Phys. Rev. B **37**, 965 (1988).
[25] A. Rubio, L. C. Balbas, and J. A. Alonso, Phys. Rev. B **46**, 4891 (1992).
[26] F. Stern, Phys. Rev. Lett. **18**, 548 (1967); T. Ando, A. B. Fowler, and F. Stern, Rev. Mod. Phys. **54**, 437 (1982), and references therein.
[27] J. B. Xia and B. F. Zhu, *Semiconductor Superlattice Physics* (Science and Technology, Shanghai, 1995).
[28] E. Skuras, R. Kumar, R. L. Williams, R. A. Stradling, J. E. Dmochowski, E. A. Johnson, A. Mackinnon, J. J. Harris, R. B. Beall, C. Skierbeszewski, J. Singleton, P. J. van der Wel, and P. Wisniewski, Semicond. Sci. Technol. **6**, 535 (1991).